

RESEARCH

Open Access



Integrative physiological and metabolic traits reveal the mechanisms of chamomile flowers in response to nicotine stress

Peng Zhou^{1†}, Qi Luo^{1†}, Dongying Pang¹, Yanhong Zhang¹, Meng Jia¹, Xuanquan Zhu¹, Yuxiang Bai¹, Xiangyun Li¹, Ge Wang^{1*}, Na Wang^{1*} and Yu Du^{1*}

Abstract

Background Chamomile (*Matricaria recutita* L.) is an important economic crop after tobacco (*Nicotiana tabacum* L.) cultivation. The nicotine released into the soil during tobacco cultivation has an impact on various aspects of chamomile growth, including plant height, flowering period, flower yield, and flower quality. We aimed to examine the effects of physiological and metabolic response of chamomile under different concentrations of nicotine stress.

Results The study revealed that chamomile growth was positively influenced by nicotine concentrations of 1.0 µg/g (N-1) and 10.0 µg/g (N-10). However, higher nicotine concentrations of 100.0 µg/g (N-100) and 500.0 µg/g (N-500) were found to induce stress as the highest levels of antioxidant enzyme activities and malondialdehyde (MDA) levels were observed under this treatment. In addition, it was observed that nicotine was transported from the roots to other organs during the entire growth period of chamomile and the nicotine levels reached saturation under N-100 treatment. A total of 1096 metabolites were detected by ultra-high-performance liquid chromatography-coupled tandem mass spectrometry (UHPLC–MS/MS) analysis, and 48 differentially expressed metabolites (DEMs) were identified among the groups via widely targeted metabolomics studies. The response of chamomile flowers to nicotine stress is associated with the presence of flavonoids, phenolic acids, organic acids, and other substances. Metabolic regulation under nicotine stress primarily involves processes, such as aminoacyl-tRNA biosynthesis, ABC (ATP-binding cassette) transporter activity, glyoxylate and dicarboxylate metabolism and pyrimidine metabolism.

Conclusions This report presents the first findings on how nicotine affects the metabolism of chamomile. It also provides a comprehensive understanding of how crops can resist nicotine stress from a metabolic perspective.

Keywords Nicotine, Chamomile, Metabolomics, Abiotic stress, Antioxidant enzyme

[†]Peng Zhou and Qi Luo have contributed equally to this work.

*Correspondence:

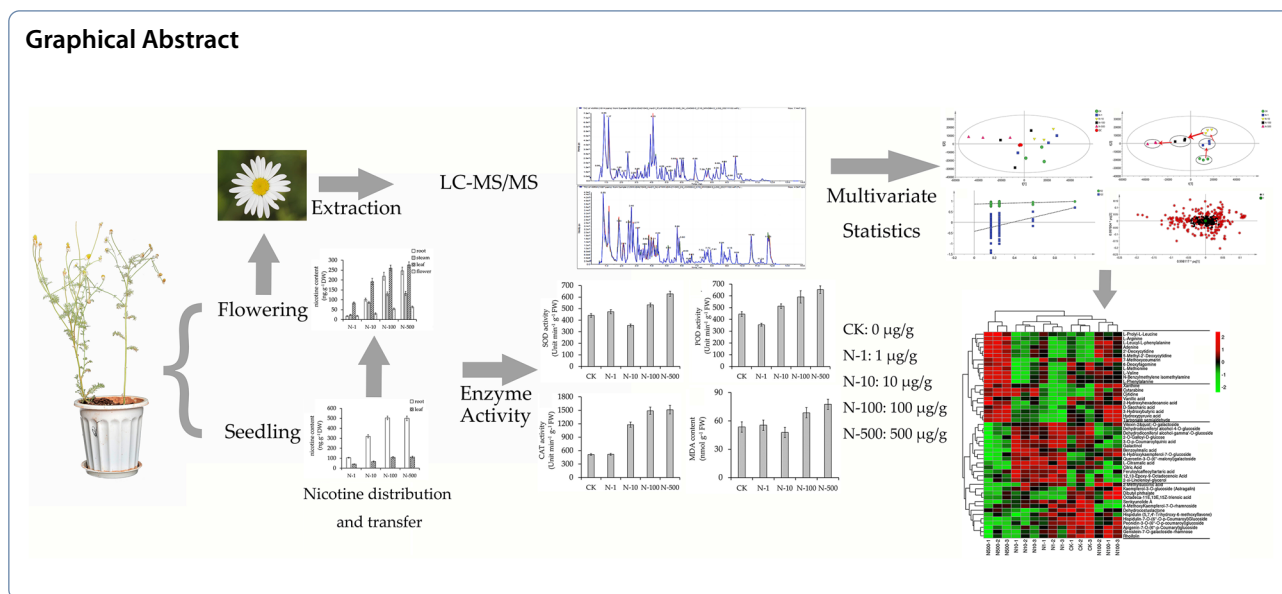
Ge Wang
wangge302@126.com

Na Wang
cindy_0725@126.com

Yu Du
duyu@ynau.edu.cn

Full list of author information is available at the end of the article





Introduction

Chamomile (*Matricaria recutita* L.), also known as mother chrysanthemum, belongs to the **Asteraceae** family and is an annual herb with sweet, fruity, and slightly bitter flowers. It is widely used in the spice and food industries [1, 2]. Chamomile flowers are abundant in chamazulene and α -bisabolol, which possess antibacterial, anti-inflammatory, wound healing, and mood-regulating properties. Consequently, they are frequently employed for medicinal purposes [3]. Chamomile is rich in flavonoids, including apigenin, luteolin, and their aglycones, which have strong antioxidant activity. As a result, they are frequently used in the production of cosmetics [4].

Tobacco is a globally valuable cash crop, with approximately 4.5 million hectares of land dedicated to its cultivation, producing approximately 6 million tons [5, 6]. During the cultivation process, a portion of the nicotine synthesized by the root system is released into the soil, and the leaching of tobacco wilting as well as the return of tobacco waste to the field can also introduce nicotine into the tobacco-growing soil. Furthermore, crops can absorb and transport nicotine, leading to damage to the soil microenvironment and compromising the quality and safety of subsequent crops [7]. Research on the effects of nicotine on plants has shown that it can cause oxidative stress response in cells and alter protein content [8], thus resulting in reduced yields of maize (*Zea mays* L.) [9] and affecting the taste of broad bean (*Vicia faba* L.), as well as the phenotype of pepper (*Capsicum annuum* L.) [10, 11]. If other crops are planted in the soil after tobacco planting, the residual nicotine in the soil can affect the quality of the planted crops and pose food safety risks.

Chamomile is a popular crop for post-tobacco planting as it helps to improve the soil microenvironment, increase land utilization, and boost the economic benefits of tobacco farmers. However, it is important to note that chamomile is sensitive to abiotic stress, such as heavy metals, heat damage, cold damage, and natural poisons. These factors can easily affect the quality of its essential oil [12, 13]. Therefore, the presence of nicotine in soil can potentially affect the primary and secondary **metabolisms** of chamomile. However, current studies are mainly focusing on exploring the sensory, phenotypic, and physiological characteristics of crops after tobacco use [10, 11].

To the best of our knowledge, this investigation represents the first attempt to elucidate the metabolic mechanism underlying the response of varieties of chamomile to nicotine-induced stress. Based on the phenotype and physiological characteristics of chamomile under nicotine stress, the metabolic response of chamomile to nicotine stress after tobacco planting was analyzed using a broadly targeted metabolomics approach. The objective of this study was to examine the effects of physiological and metabolic response of chamomile under different concentrations of nicotine stress. The findings of this study can provide useful insights into the mechanism of crop responses to nicotine stress.

Materials and methods

Plant materials and reagents

Deionized water was prepared by a Milli-Q water purification system (Millipore, Bedford, MA, USA). LC-MS grade acetonitrile, methanol, formic acid and nicotine

(Purity > 99.9%) were purchased from Merck (Darmstadt, Germany).

Chamomile seeds were purchased from Muxi Vanilla Plantation, Shangqiu City, Henan province, China. Nicotine concentration gradients were divided into five sample groups based on field measurements of nicotine in tobacco-growing soil for different years of continuous cropping: 0 µg/g (CK), 1.0 µg/g (N-1), 10.0 µg/g (N-10), 100.0 µg/g (N-100) and 500.0 µg/g (N-500). The red soil was utilized in our experiment with pH 6.3, which was commonly employed for tobacco cultivation, and the alkali-hydrolyzable nitrogen, available phosphorus, available potassium, and organic matter (OM) contents of 176.1, 135.8, 143.9 and 44.0 µg/g, respectively. The native soil was screened and mixed with fine sand. Chamomile seedlings were cultivated in a 1:3 sand–soil mix. Afterwards, chamomile seedlings with uniform growth were carefully chosen and transplanted into plastic pots measuring 15 cm in diameter and 25 cm in height. After the seedlings were stabilized for 7 days, varying concentrations of nicotine solution were applied evenly to the soil only once and pure water was used as control (CK). Each pot contained two plants and three biological replicates were collected. During this period, the flowering time, the number and weight of flowers were recorded.

Analysis of antioxidant enzyme activities and lipid peroxidation product content

The measurement of indicators of the antioxidant enzyme system includes evaluating the levels of superoxide dismutase (SOD), peroxidase (POD), catalase (CAT), and the lipid peroxidation product malondialdehyde (MDA), which were measured according to Lei et al. [14].

Determination of nicotine content in various organs of chamomile

Samples preparation

Samples of various organs of chamomile (seedling organs include root and leaf; flowering organs include root, stem, leaf, and flower) were collected separately. The samples were quickly frozen in liquid nitrogen and then ground and crushed in a mortar. The resulting material was transferred to a 50 mL frozen centrifuge tube and then lyophilized for 48 h in a freeze dryer (vacuum 18 Pa, temperature – 6 °C). Finally, the samples were stored in a – 80 °C ultra-low-temperature refrigerator. Nicotine content in plants was adjusted appropriately according to the method of Lozano et al. [7]. Briefly, the above samples were accurately weighed 6.00 g and transferred into a 50 ml centrifuge tube, moistened with 5% NaOH solution and incubated for 15 min. Then, 30 mL of a 0.01% triethylamine–methyltert-butyl ether solution was added

into each tube and extracted with sonication for 20 min. After centrifugation at 6000 rpm for 5 min, 10 mL of the organic phase was transferred to a KD bottle and concentrated to 1 mL at 35 °C using a rotary evaporator. For purification, 0.5 g of anhydrous sodium sulfate and 20 mg of primary secondary amine (PSA) filler were added and allowed to stand for 15 min. The mixture was filtered through a 0.22 µm polytetrafluoroethylene (PTFE) filter and the filtrate was transferred to a 2 mL brown sample vial for gas chromatography–mass spectrometry (GC–MS) analysis.

GC–MS analysis

The samples were analyzed by an Agilent 5977B MSD mass spectrometer coupled to an Agilent 7890B GC (Agilent Technologies, USA) and equipped with an HP-5MS capillary column (30 m × 0.25 mm × 0.25 µm). Separation was achieved with a temperature program of 70 °C, and then increased to 120 °C and 260 °C at constant ratios of 5 °C/min and 1 °C/min, respectively. The oven was kept at 260 °C for 7 min and the inlet temperature were held at 250 °C. The flow rate of high-purity helium gas (≥ 99.999%, China) was 1.1 mL/min and the injection volume was 2 µL. The Collision energy was 70 eV. The temperatures for the ion source and MS transfer lines were maintained at 230 °C and 280 °C, respectively. The scanning mode was selected ion monitoring (SIM), while the scanning speed was optimized to 5 spectra/s. The solvent delay was set to 6.0 min.

Widely targeted metabolomics analysis

Samples preparation and extraction

For metabolomics detection by UHPLC–MS/MS, fresh chamomile flowers, including stamens, pistils, petals, calyxes, receptacles, and ovaries, were collected by cutting them from the flower stem, snap-frozen in liquid nitrogen, ground, and pulverized. The material was transferred to a 15 mL frozen centrifuge tube and stored at a temperature of – 80 °C in an ultra-low-temperature refrigerator. Samples were processed and extracted as reported previously [15, 16]. Briefly, 100 mg freeze-dried sample powder was weighed and added into 1.0 mL 70% methanol solution and extracted at 4 °C for 24 h. After centrifuging at 10000 r/min for 10 min, the supernatant was injected into a Vanquish UHPLC system (UHPLC, SHIMADZU CBM30A; MS/MS, Applied Biosystems 6500 QTRAP). In the course of instrumental analysis, quality control (QC) samples were generated by pooling equal volumes amounts of sample extracts. To ensure the consistency and accuracy of the analysis process, one QC sample was included for every 5 test analysis samples to evaluate the repeatability of the analytical process.

UHPLC–MS/MS analysis

The samples were analyzed using UHPLC–MS/MS system based on the previously reported instrument parameter setting [15, 17]. The liquid chromatographic separation was achieved on a Waters ACQUITY UPLC HSS T3 column (2.1×100 mm, 1.8 μm). The UHPLC system employed a mobile phase composed of 0.04% acetic acid in water (A) and 0.04% acetic acid in acetonitrile (B). The solvent gradient program was set as follows: 95% A (0 min), 5% A (11.0 min), 5% A (12.0 min), 95% A (12.1 min), 95% A (15.0 min). The column oven temperature was set at 40 °C, and the flow rate was maintained at 0.4 mL/min. The injection volume was 2 μL. The effluent was connected to an ESI–triple–quadrupole–linear ion trap (QTRAP)–MS. API 6500 Q-TRAP UHPLC/MS/MS System was operated in both positive and negative ion mode. The ESI source operation parameters were as follows: ion source, ESI turbo spray; source temperature 550 °C; Ion spray voltage (IS) 5500 V (positive ion mode)/– 4500 V (negative ion mode); Curtain gas (CUR) was set at 25.0 psi. The collision-activated dissociation was high. Declustering potential (DP) and collision energy (CE) for individual MRM transitions were done with further DP and CE optimization. For each period, a specific set of MRM transitions were monitored based on the metabolites that were eluted during that period.

Data analysis

The raw data files generated by UHPLC–MS/MS were processed using Analyst 1.6.1 (AB SCIEX). Principal component analysis (PCA) and Orthogonal Partial Least

Squares–Discrimination Analysis (OPLS–DA) were performed using SIMCA software (14.1 version, Umetrics AB, Umea, Sweden). The quality and reliability of models are typically evaluated using three parameters: R^2X , R^2Y , and Q^2 . If the values of these parameters are close to 1.0, it indicates that the model has excellent fitting and predictive capability [18]. Kruskal–Wallis nonparametric test and significance test were analyzed using SPSS 26.0 software (IBM, Chicago, USA). Potential markers were screened by the combination of variable importance in projection (VIP) value ($VIP > 1$) and Kruskal–Wallis nonparametric test ($p < 0.05$) [19]. Hierarchical cluster analysis (HCA) and heat map analysis (HMA) performed with Multiexperiment Viewer 4.9.0 software (J. Craig Venter Institute, La Jolla, CA, USA). MBROLE 3.0 (<http://csbg.cnbc.csic.es/mbrole3/>) and the Kyoto Encyclopedia of Genes and Genomes (KEGG) pathway database were utilized to analyze metabolic pathway enrichment (<https://www.kegg.jp/kegg/pathway.html>). The significance was determined by hypergeometric test threshold p values.

Results

The effect of nicotine treatment on the plant phenotypes, flowering time and number

Nicotine showed significant effects on the phenotypes of chamomile both seedlings and flowering stages, with varying performance depending on the concentration. Chamomile growth was enhanced during the seedling stage under the N-1 and N-10 treatments (Fig. 1A). However, the plants showed yellowish leaves under N-1 treatment, whereas showed the most favorable growth

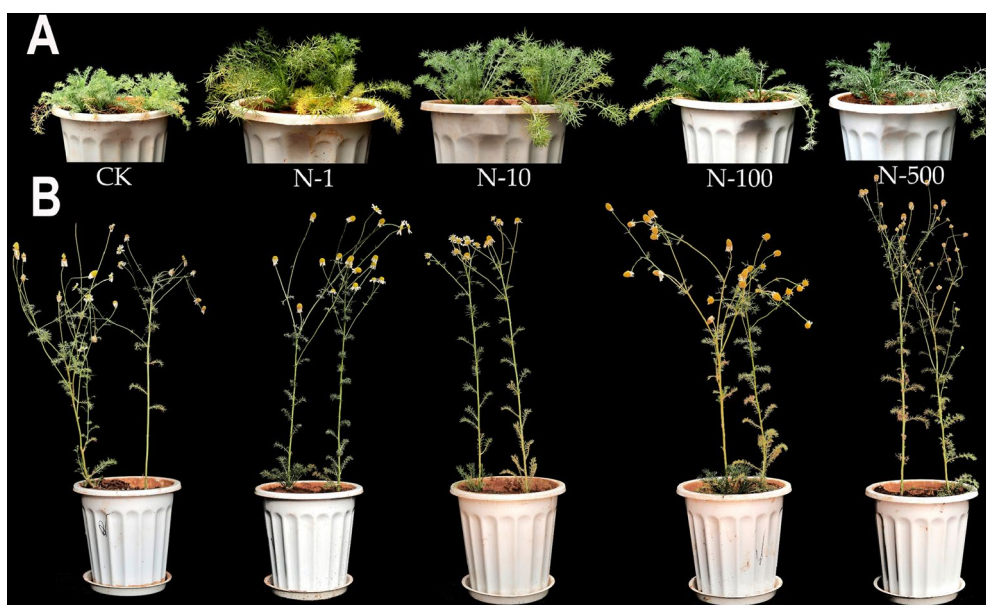


Fig. 1 Phenotypes of chamomile under nicotine stress. Seedling phenotype (A); flowering phenotype (B)

status after N-10 treatment. On the other hand, plants subjected to N-100 and N-500 treatments were shorter and displayed a growth pattern similar to the CK. As for flowering stage (Fig. 1B), chamomile flowers normally under all treatments during the flowering stage. Compared to the CK, flowers exposed with N-100 and N-500 displayed smaller size, faster fading, and withered leaves. However, when treated to lower concentrations (N-1 and N-10), the plants exhibited positive growth with green, yellow, and white colors, and did not experience withering. There was no significant difference observed between the treatment groups and the CK. As the nicotine concentration increased, there was a noticeable increase in leaf shedding and flower decay.

Nicotine showed significant effects on flowers (Table 1). With the increase in nicotine concentration, the flowering time of chamomile was delayed compared with CK. The most obvious was that the flowering period was delayed by 9 and 10 days under N-100 and N-500, respectively, and the number and weight of flowers showed a decreasing trend. Compared with CK, the number and the weight of flowers were insignificant under N-1 and N-10. But decreased significantly by more than half and decreased significantly by 30.1% under N-500.

Response of chamomile antioxidant system and MDA content under nicotine

The activity of antioxidant enzymes in plants can be enhanced to maintain plant life under unfavorable conditions. Superoxide dismutase (SOD) levels were significantly higher in the N-100 and N-500 treatments compared to the control group (CK). Similarly, peroxidase (POD) and catalase (CAT) levels were also highest in the N-100 and N-500 treatments (Fig. 2). These findings suggest that the chamomile antioxidant system is activated in the presence of high nicotine concentrations, enabling antioxidant enzymes to facilitate normal plant growth. In this study, elevated levels of MDA, the product of membrane lipid peroxidation, were observed in both N-100 and N-500 treatments.

Content of nicotine in chamomile plants in different periods

Based on the phenotypic characteristics and plant antioxidant system, it was confirmed that the plant was indeed under stress. Subsequently, we conducted a comprehensive investigation of the distribution of nicotine in chamomile at different growth stages. Nicotine was primarily concentrated in the roots, with a smaller portion being transported to the leaves (Fig. 3A). Furthermore, as the concentration of nicotine increases, the accumulation of nicotine in both the roots and leaves of chamomile also increased. It was observed that the plant reaches a saturation point for nicotine accumulation when the concentration reaches 100 $\mu\text{g/g}$. The distribution of nicotine in chamomile plants at the flowering stage in comparison with the seedling stage, nicotine was transported to other organs through the root system. The accumulation of nicotine in the root system was relatively decreased, while the accumulation in the leaves was relatively increased (Fig. 3B). In addition, it implies that low-concentration of nicotine treatment has a positive effect on the growth of chamomile during the seedling stage (Fig. 1A). However, plants treated with high concentrations of nicotine during the flowering stage exhibited yellow stems, withered leaves, and early flower decline (Fig. 1B).

Widely targeted metabolomics analysis

The chromatograms of samples collected under MRM mode on UHPLC–MS/MS platform are shown in Fig. 4A (positive ion mode) and Fig. 4B (negative ion mode). The overlap of total ion flow chromatograms detected by metabolites in QC samples were high (Fig. 4C, D), indicating that the data obtained in the experiment had good repeatability and high reliability.

Univariate analysis

Kruskal–Wallis test demonstrated significant differences in the metabolites ($p < 0.05$), indicating that they may serve as the distinctive metabolites of chamomile under the stress of nicotine. Compounds with a relative standard deviation (RSD) greater than 30% were excluded. The remaining 1096 compounds later analyzed, and

Table 1 Effects of different concentrations of nicotine treatment on flowers

treatment	flowering time (days after transplanting)	number of flowers/plant (mean \pm SD)	dry weight (g/100 flowers, mean \pm SD)
CK	55	21 \pm 2a	22.5 \pm 1.2a
N-1	56	22 \pm 2a	23.9 \pm 1.4a
N-10	59	21 \pm 1b	22.9 \pm 1.2a
N-100	64	12 \pm 2c	16.9 \pm 0.9b
N-500	65	10 \pm 2c	15.7 \pm 1.1b

Different lowercase letters indicate significant differences under different nicotine concentrations according to the significance test at $P < 0.05$

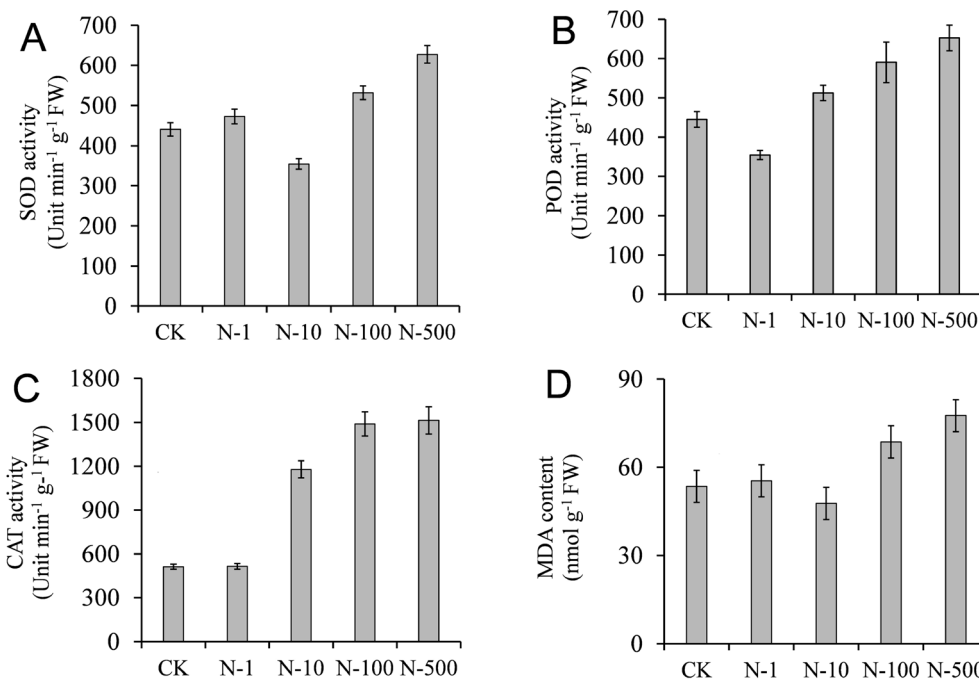


Fig. 2 Effects of different concentrations of nicotine treatment on antioxidant oxidase activity and malondialdehyde content in chamomile leaves. The enzymatic activity of superoxide dismutase (SOD) (A); the enzymatic activity of peroxidase (POD) (B); the enzymatic activity of catalase (CAT) (C); malondialdehyde (MDA) content (D)

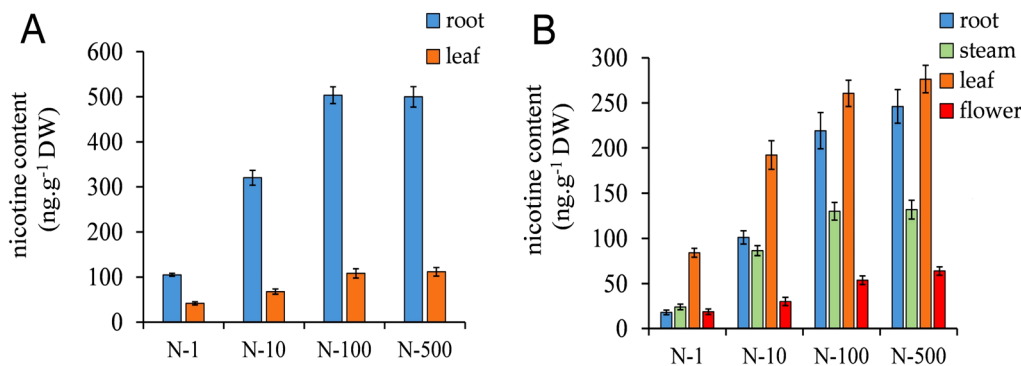


Fig. 3 Dynamic distribution of nicotine in chamomile plants. Distribution of nicotine in plants at seedling stage (A); distribution of nicotine in plants at flowering stage (B)

they consisted of 24.3% flavonoids, 17.9% phenolic acids, 12.4% lipids, 8.7% amino acids and their derivatives, 7.1% organic acids, 5.6% lignans and coumarins, 5.2% nucleotides and their derivatives, 4.4% alkaloids, 4.2% terpenes, and 9.6% other compounds. Out of these, 13 compounds were found to overlap ($p < 0.05$) in four groups of comparative samples (Fig. 5). This indicates that there were significant changes in these compounds after treatment with different concentrations of nicotine. Notably, the concentration of N-500 resulted in the highest level of stress, leading to the greatest number of significantly

changed compounds. Conversely, the low concentration of N-1 treatment resulted in the least number of compounds with significant changes.

Multivariate analysis

Unsupervised PCA of sample data was conducted after normalization using pareto scaling method. Figure 6A shows the 2D scatter plot of the scores of PC1 versus PC2, together explaining 43.4% of the total variance (31.7% and 11.7%, respectively). The QC samples were located in the center of the PCA scores plot, demonstrating the

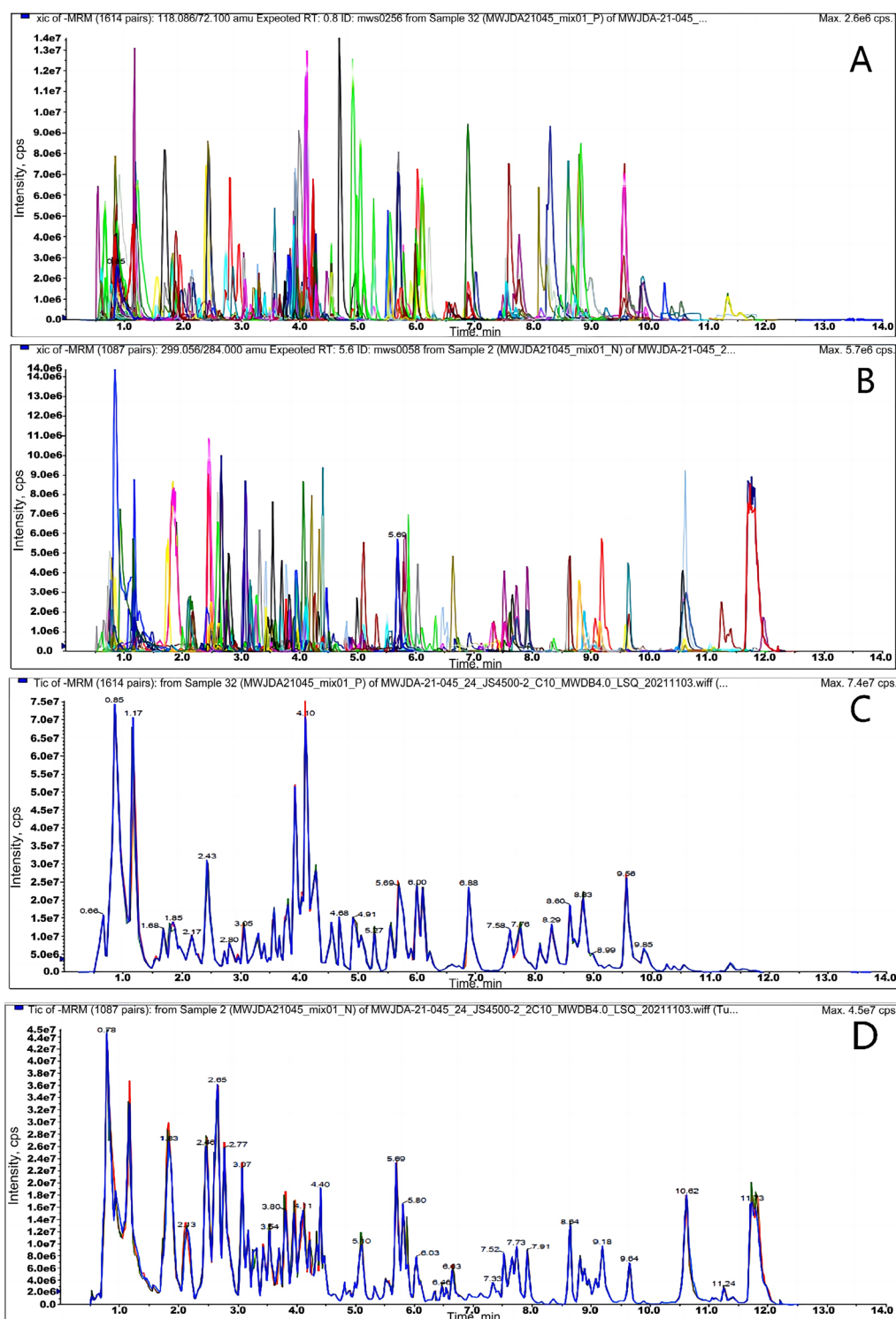


Fig. 4 Multi-peak of metabolite detection and QC sample mass spectrometry detection TIC overlay. Multi-peak of metabolite detection under positive ion mode (A); multi-peak of metabolite detection under negative ion mode (B); QC sample mass spectrometry detection TIC overlay under positive ion mode (C); QC sample mass spectrometry detection TIC overlay under negative ion mode (D)

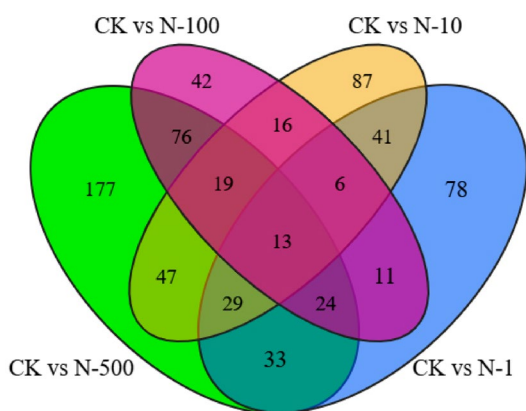


Fig. 5 Venn diagram showing the overlapping and accession-specific differential metabolites among the comparison groups (CK: 0 µg/g; N-1: 1 µg/g; N-10: 10 µg/g; N-100: 100 µg/g; N-500: 500 µg/g)

effectiveness of the data analysis strategies. In addition, samples treated with varying nicotine concentrations were partially distinguishable from each other. However, the PCA (R^2X (cum) = 0.531, Q^2 (cum) = 0.125) predictive accuracy was deemed unsatisfactory. Advanced statistical analysis methods should be employed to attain superior results. As some useful discriminate information may have been missed during feature extraction and dimension reduction of the data. An improved and better discrimination of metabolites was achieved by performing supervised OPLS-DA analysis. (Fig. 6B). The explanatory and predictive power of the model was greatly improved (R^2X = 0.723, Q^2 = 0.549), and the difference between groups were more obvious. As the nicotine concentration increased, the samples in each group exhibited a counterclockwise shift from CK to N-500. (Direction of red arrow). A cross validation analysis showed the Q^2 and R^2 intercepts were -0.448 and 0.769, respectively (Fig. 6C). Demonstrating that OPLS-DA model is reliable, not overfitted, and describes the samples classification well.

Differential expressed metabolites screening

In total, 48 metabolites (VIP > 1, $p < 0.05$) (Fig. 6D), including flavonoids (22.9%), organic acids (14.58%) and phenolic acids (14.58%), amino acids and their derivatives (12.50%), nucleotides and derivatives (12.50%) etc., were tentatively identified (Additional file 1: Table S1).

To intuitively reflect the changes of DEMs under different treatments, in this experiment, HMA was employed and HCA was utilized to perform correlation analysis. A metabolite heat map was generated using clustering features (metabolites) and variables treatments (Fig. 7). The clustergrams were presented as color blocks to represent each participant's row of data across each column of variables, with red boxes indicating higher levels and green

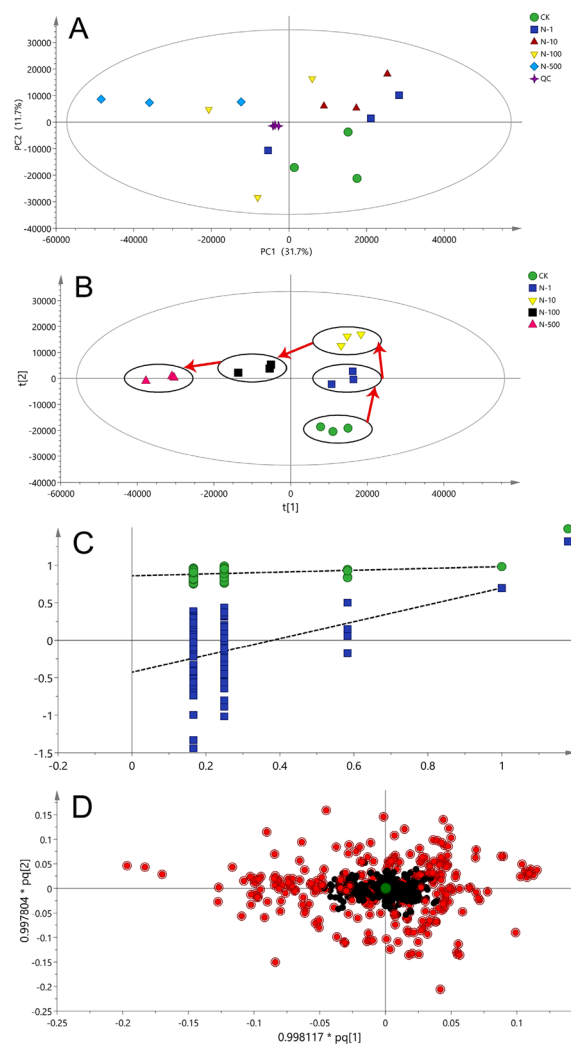


Fig. 6 Multivariate statistical analysis of chamomile samples treated with different nicotine concentrations (CK: 0 µg/g; N-1: 1 µg/g; N-10: 10 µg/g; N-100: 100 µg/g; N-500: 500 µg/g; QC: quality control). PCA score plot R^2X (cum) = 0.513, Q^2 (cum) = 0.125 (A); OPLS-DA score plot, R^2X (cum) = 0.723, Q^2 (cum) = 0.549 (B); cross-validation plot of OPLS-DA model with 200 permutation tests (intercepts of Q^2 and R^2 were -0.448 and 0.769, respectively) (C); loadings plot of OPLS-DA (red squares represent the most differential metabolites) (D)

boxes indicating lower levels of metabolites. According to the trend of change, 48 compounds were divided into two classes (first class: groups A and B, second class: groups C and D).

The first class, including groups A and B, primarily consists of amino acids and their derivatives, nucleotides and their derivatives, and organic acid compounds. In addition, there was a small amount of alkaloids, such as 6-deoxyfagomine and N-benzylmethylene isomethylamine, as well as coumarins such as

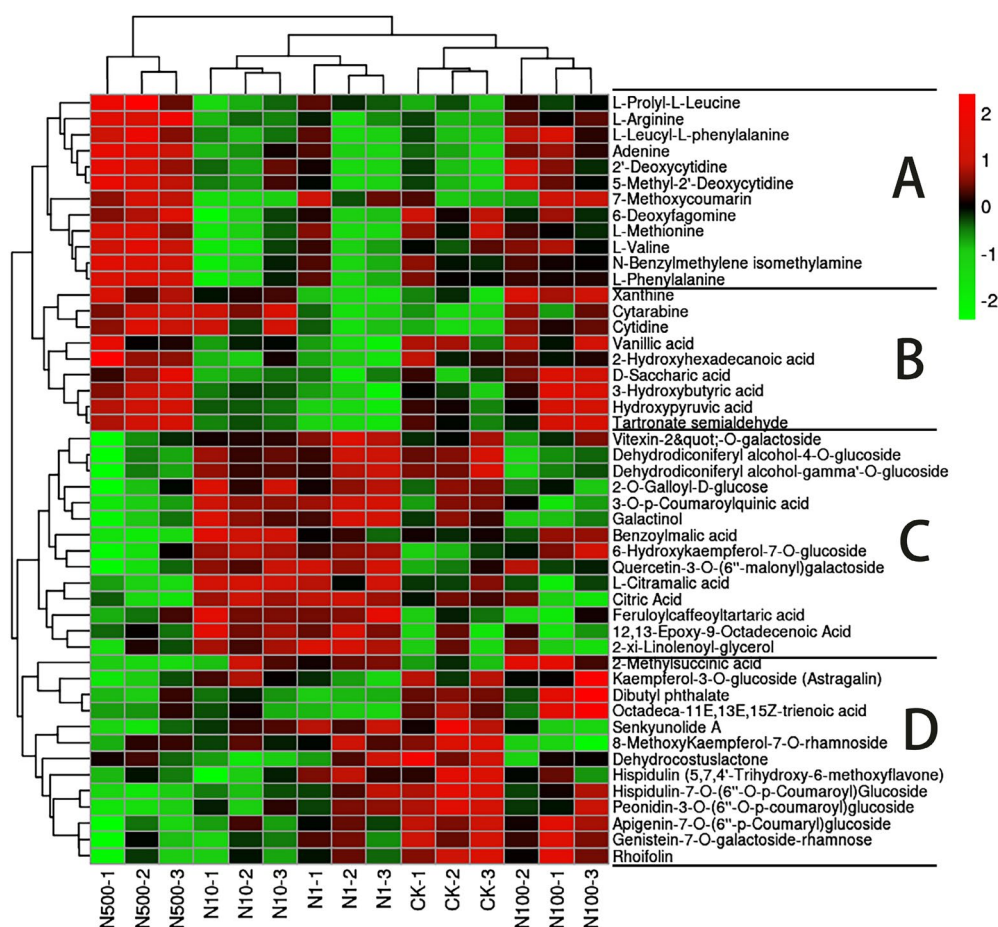


Fig. 7 HMA and HCA analyses of metabolite contents under various concentration of nicotine. Red represents high content, while green represents low content

7-methoxycoumarin and phenolic acids, such as vanillic acid. The variations in content among group A differentially expressed DEMs across distinct treatment samples were as follows: the levels of 7-methoxycoumarin and six other metabolites were found to be higher in the samples than in the samples treated with CK (control), and there was a tendency for the levels of 7-methoxycoumarin and six other metabolites to decrease and then increase as the concentration of nicotine treatment increased. The highest content was observed in N-500 samples. The content of L-prolyl-L-leucine and other 6 metabolites were low under relatively low concentrations of nicotine (N-1, N-10) treatment, and increased in N-100 treatment, and the highest content in N-500 treatment, showing an increasing trend. Group B was mostly organic acids and nucleotides and their derivatives. The content of group B was higher under N-100 and N-500 treatment, and the content of group B was lowest under N-1 treatment.

The second-class including group C and D were mostly phenolic acids and flavonoids, among them, the content of group C differential metabolites were higher in N-1 and N-10, and the lowest in N-100 and N-500. The content of group D compounds were the highest in CK, and showed a gradually decreasing trend with the increase of nicotine concentration.

The KEGG metabolic pathway analysis of DEMs

The 48 DEMs were matched with KEGG compound IDs of plant metabolites, and the results were mapped to MBROLE 3.0 for KEGG enrichment analysis. Pathway database of KEGG was used for metabolic pathway analysis of the enriched pathways. Based on the mapping results, 19 pathways were provided (hypergeometric test threshold $p < 0.05$) (Fig. 8), including aminoacyl-tRNA biosynthesis, metabolic pathways, glyoxylate and dicarboxylate metabolism, biosynthesis of alkaloids derived from ornithine, lysine and nicotinic acid, biosynthesis of plant hormones, glucosinolate biosynthesis, ABC

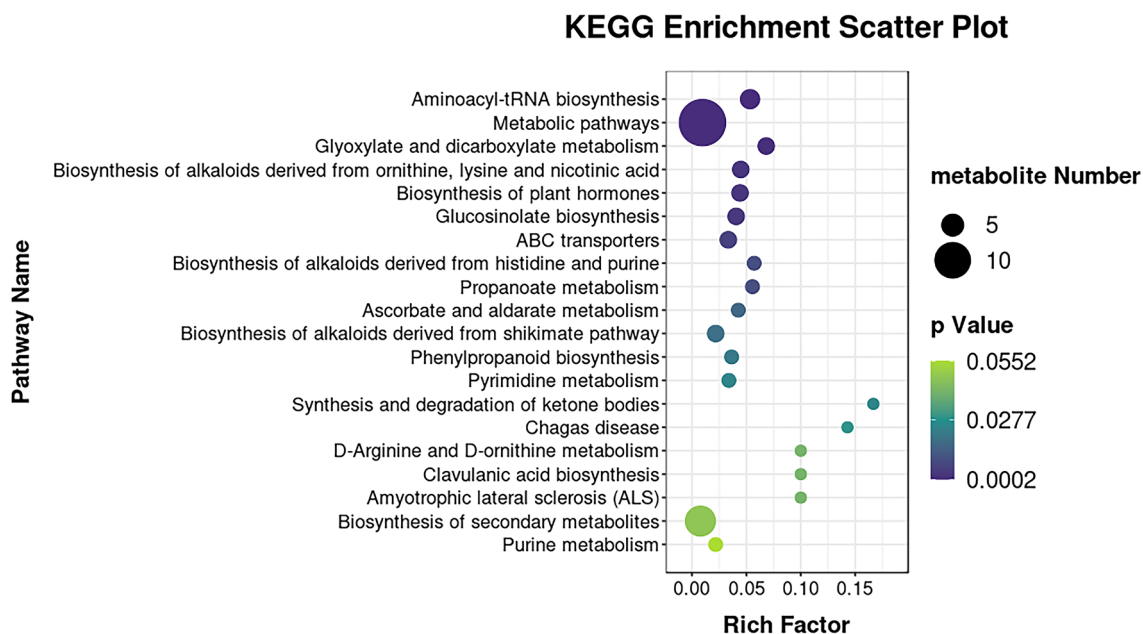


Fig. 8 Bubble plot of differential metabolites enriched in metabolic pathways of chamomile. The color of the bubble indicates the p value of enrichment analysis. The size of the bubble indicates the number of metabolites in this pathway

transporters, biosynthesis of alkaloids derived from histidine and purine, propanoate metabolism, ascorbate and aldarate metabolism, biosynthesis of alkaloids derived from shikimate pathway, phenylpropanoid biosynthesis, pyrimidine metabolism, synthesis and degradation of ketone bodies, chagas disease, D-arginine and D-ornithine metabolism, clavulanic acid biosynthesis, amyotrophic lateral sclerosis (ALS) and biosynthesis of secondary metabolites.

The response of amino acids and their derivatives in the aminoacyl-tRNA biosynthesis are shown in Fig. 9A. These metabolites were the highest in N-500 samples and were considered to be the key substances in the aminoacyl-tRNA biosynthesis. Citric acid was involved in the ascorbate and aldarate metabolism in glyoxylate and dicarboxylate metabolism. The changes in the levels of these three organic acids in the pathway under gradient nicotine treatment (Fig. 9B). The variation trend of hydroxy pyruvic acid and tartronate semialdehyde was opposite to that of citric acid, and the tendency of accumulation occurs at high nicotine concentration. Nucleotide compounds were involved in the biosynthesis of alkaloids derived from purine and pyrimidine metabolism, the changes of three nucleotides involved in purine and pyrimidine metabolism are shown in Fig. 9C, which showed high accumulation at high concentrations (N-100 and N-500). The accumulation of amino acids and derivatives, nucleotides and derivatives, and organic acids under abiotic stress has been studied, but

the relationship between the three types was not clear. In this study, we performed Pearson correlation analysis to investigate the association between the expression levels of three types of compounds, with the aim of characterizing the correlation patterns of these compounds in their respective pathways. As shown in Fig. 9D, citric acid and L-citramalic acid were significantly negatively correlated with the expression of other compounds, while 2-methylsuccinic acid in response to nicotine stress was negatively correlated with other substances additionally, in response to stress, the expression levels of nucleotides and derivatives were always positively correlated with amino acids, and cytarabine was strongly correlated with homogeneous compounds. However, the correlation with the expression of amino acids and their derivatives and organic acids was not significant.

Discussion

Phenotypic characteristics and enzyme activity respond to nicotine stress

When plants were under stress, they exhibit various symptoms, such as yellowing and wilting of leaves, leaf fall [20], delayed flowering time, withered stamens and pistils, and smaller flowers [21, 22]. These responses may be the strategies employed by chamomile to ensure its survival and reproduce quickly [23]. Surprisingly, similar to the accumulation pattern observed during the seedling stage, the nicotine content in the root, stem, leaves, and flowers reaches saturation point at N-100 during the

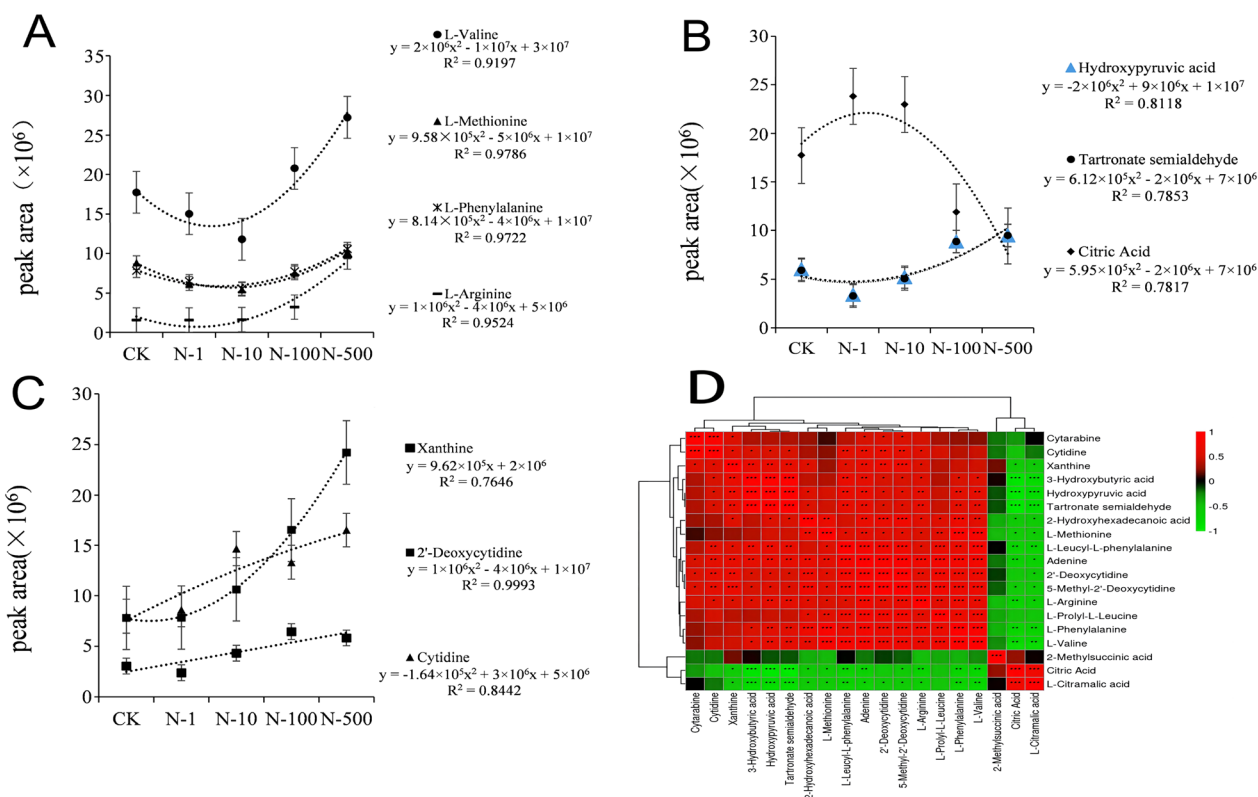


Fig. 9 Response curve fitting diagram of amino acids and their derivatives in the aminoacyl-tRNA biosynthesis under different nicotine concentrations (A); response curve fitting diagram of organic acids in glyoxylate and dicarboxylate metabolism under different nicotine concentrations (B); response curve fitting diagram of nucleotides and their derivatives in biosynthesis of alkaloids derived from histidine and purine, pyrimidine metabolism under different nicotine concentrations (C); the associated expression of amino acids and their derivatives, nucleotides and their derivatives, organic acids, red box means positive correlation, green box means negative correlation (* represents significance $p < 0.05$, ** represents significance $p < 0.01$, *** represents significance $p < 0.001$, based on Pearson correlation test) (D)

flowering stage. Further increase in treatment concentration did not result in any change in the nicotine content. This finding supports the idea that the presence of nicotine in the leaves and stems enhances the antioxidant capacity of these organs. This phenomenon could be attributed to the absorption of nicotine by chamomile during the seedling stage, which is then transported to various plant organs such as leaves and flowers as the plant matures and accumulates the substance (Fig. 3A, B), which may also be the cause of delayed flowering time and decreased flower yield [24, 25]. Nicotine entered the plant through root cells and gradually accumulated in target organs, thereby impacting crop quality, which was further evidenced by the increased activity of antioxidant enzymes and levels of MDA. These substances play a crucial role in maintaining the homeostasis of reactive oxygen species by scavenging free radicals when plants are under stress [26]. MDA, a key product of cell membrane lipid peroxidation, serves as an indicator of stress due to its increased content (Fig. 2) [27].

DEMs and major pathways in response to nicotine stress

A total of 1096 metabolites were detected by UHPLC-MS/MS, out of which 48 differential metabolites were identified using multivariate statistical analysis. These included flavonoids (22.9%), organic acids (14.58%), phenolic acids (14.58%), amino acids and their derivatives (12.50%), nucleotides and derivatives (12.50%). Flavonoids would express resistance to abiotic stress, and their content would be increased by promoting their synthesis through enzymes with flavonoid synthesis, and their high accumulation shows stronger tolerance to abiotic stress [28]. Studies showed that the content of flavonoids was higher than that of normal conditions when soybean was under drought stress, the more severe the stress was, the higher the content was. Wolfberry (*Lycium chinese*) also showed high accumulation of flavonoids under salt stress [29, 30]. In chamomile flowers, the content of flavonoids increased at N-1 and N-10, but decreased at N-500. In our study, the content of flavonoids was reduced because of consumption or inhibition of synthesis in N-100 and N-500, which was the direct cause of the decline in the

medicinal quality of chamomile. In addition, due to the stress from nicotine, plants were genetically conserved, and flowers withered when they were not fully mature, which may also be the reason for the decline in the quality of chamomile flowers. Therefore, the study showed that the application of nicotine in N-1 and N-10 had no significant effect on the medicinal value of chamomile. The specific situation needs to be further studied.

Amino acids and their derivatives together with organic acids (except L-citramalic acid, citric acid, 2-methylsuccinic acid) were highest under N-500 treatment, and the expression under low-concentration (N-1 and N-10) was lower than CK. The contents of L-citramalic acid, citric acid and 2-methylsuccinic acid in N-500 and N-100 were lower than other treatments. Organic acids, amino acids and their derivatives, as a class of substances involved in physiological and biochemical regulation in plants, play an important role in resisting abiotic stress [31, 32]. Studies have shown that amino acids in plants respond to heavy metal toxic stress mainly through the formation of complexes between carboxyl and amino groups and heavy metals, and another response mechanism was the accumulation and absorption of free amino acids by asparagine and glutamine, so as to reduce ammonium salt stress [33, 34]. The response of organic acids to heavy metal ion stress often involves converting heavy metals into chelated forms, which aids in resisting cadmium stress [35]. In our study, we observed a significant increase in the metabolism of organic acids and amino acids in flowers with the concentration of nicotine treatment (except citric acid). This research has shown that these compounds and their derivatives played a regulatory role in responding to nicotine stress. Nucleotides and their derivatives were responsible for controlling the synthesis of specific proteins that help plants resist adverse environmental conditions, such as ion channel proteins, enzymes, and plant hormones. [36, 37].

Phenolic acids are major polyphenols widely found in plants, their response mechanism to abiotic stress was similar to that of flavonoids. They protect the normal physiological metabolism of plants by scavenging superoxide free radicals, and express antioxidant effects by accumulating phenolic acids [38, 39]. Our study found that the content of seven phenolic acids increased under low concentrations (N-1 and N-10) nicotine stress. Compared with CK, the content of seven phenolic acids in N-500 was lower. This decrease in content could be attributed to either a reduction in the production of phenolic acids as a response to nicotine stress or the direct impact of nicotine on the enzymes involved in the synthesis pathway of these substances [40, 41].

Studies have shown that L-valine is a metabolite that plays an important role in drought stress and improved

plant tolerance [42]. It was also reported that exogenous amino acid mixtures (including L-valine, L-methionine, L-phenylalanine, L-arginine) were used to improved drought tolerance of cabbage and improved its nutritional quality [43]. L-arginine, L-valine, and L-phenylalanine (Fig. 10) play crucial roles as key compounds in the Phosphate and amino acid transporters of the ABC transporter pathway in response to abiotic stress. These compounds were annotated in the response of chamomile to nicotine stress, indicating their involvement in secondary metabolic resistance to stress. By controlling ATP synthesis, these compounds provided the necessary energy for transmembrane transport of substances [44, 45]. In plants, these compounds were essential for maintaining cellular homeostasis and restoring metabolic balance after stress [46, 47].

The involvement of citric acid in the pathway occurred through the citric acid cycle. L-phenylalanine and L-arginine contributed to the synthesis of alkaloids derived from ornithine (Fig. 10). Citric acids content in specific crops have been reported to decrease when subjected to waterlogging and salt stress. This decrease was attributed to the degradation of citric acid and the maintenance of reactive oxygen species homeostasis, which improved the tolerance of specific crops to abiotic stress [48–50]. Ascorbate and aldarate metabolism played significant roles in plant stress resistance [51, 52]. Finally, citric acid and L-phenylalanine were key components in the pathway of biosynthesis of plant hormones (Fig. 10), particularly in the synthesis of ethylene and salicylic acid, ethylene facilitates the ripening of chamomile seeds, while salicylic acid improved the tolerance of flowers to nicotine [53, 54]. As reported that pyrimidine metabolism is often enriched when crops are subjected to abiotic stress [55, 56]. Xanthine, 2'-deoxycytidine and cytidine were mainly involved in enzyme synthesis, inducing the formation of stress resistance pathways, and were closely related to crop response to abiotic stress [27, 57].

Conclusion

In present study, we investigated the phenotype and enzyme activity of chamomile under exogenous nicotine application. We also demonstrated the dynamic accumulation of nicotine and chamomile's impact on the phenotype response to stress. Since the flower organ of chamomile holds medicinal value and economic benefits, we have analyzed the metabolomics changes in chamomile flowers treated with different concentrations of nicotine. Our results revealed that low-concentration nicotine promoted the growth of chamomile, while high-concentration nicotine caused stress. We observed that high-concentration nicotine resulted in a short flowering period, withered leaves, and yellow stems in chamomiles.

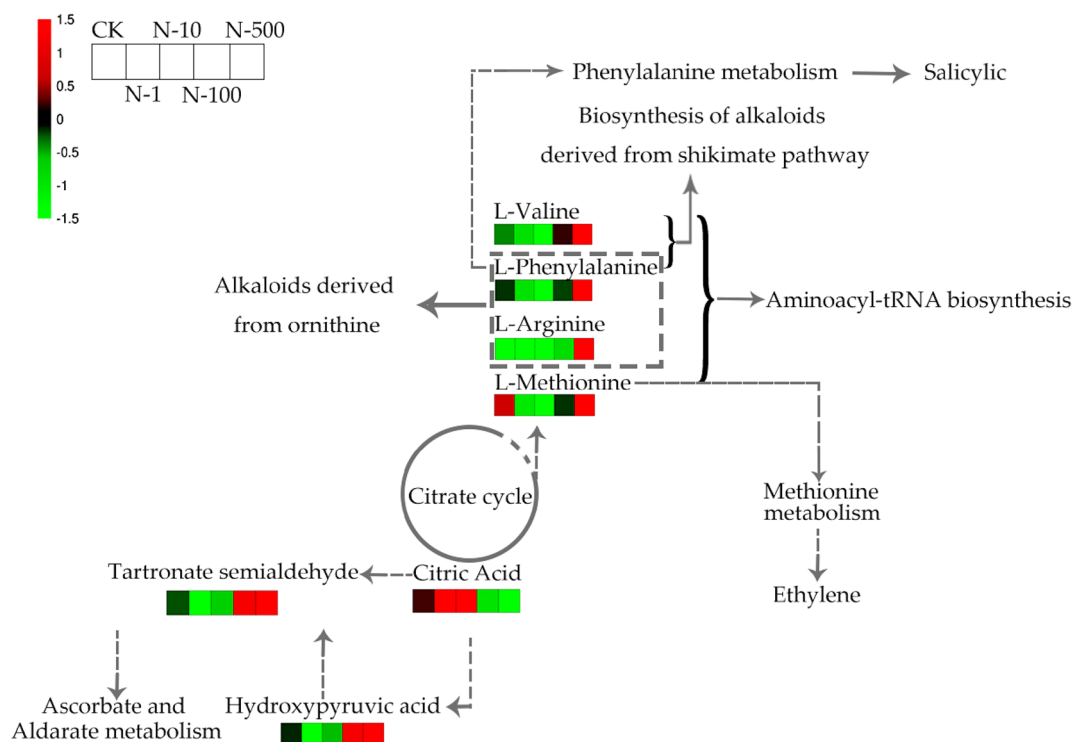


Fig. 10 Metabolic pathways of the main metabolites at different nicotine concentration treatments. Red boxes represent high nicotine content, while green boxes represent low nicotine content, the bars show the different content of metabolites from left to right in CK, N-1, N-10, N-100, N-500

It was crucial to emphasize that nicotine tended to transport from roots to other organs throughout the growth period of chamomile, as the concentration of nicotine increased, it accumulated in stems, leaves, and flowers, and ultimately reached saturation under N-100 treatment. Metabolomics analysis revealed high concentrations of nicotine (N-500) can increase the contents of amino acids and their derivatives, nucleotides and their derivatives, and organic acids (except citric acid). It was worth noting that the content of flavonoids and phenolic acids, which were the primary medicinal active ingredients in chamomile flowers, were reduced. In addition, DEMs were used to enrich the pathway of aminoacyl-tRNA synthesis, glyoxylate and dicarboxylate metabolism, and biosynthesis of alkaloids derived from histidine and purine, pyrimidine metabolism, ABC transporter, and other pathways involved in resistance to nicotine stress. Our results lay a foundation for the study of regulating metabolic characteristics of crops in response to nicotine stress.

Abbreviations

- MDA Malondialdehyde
- SOD Superoxide dismutaseperoxidase
- POD Peroxidase

- CAT Catalase
- UHPLC-MS/MS Ultra-high-performance liquid chromatography-coupled tandem mass spectrometry
- GC-MS Gas chromatography-mass spectrometry
- DEM Differentially expressed metabolite
- QC Quality control
- KEGG Kyoto encyclopedia of genes and genomes
- VIP Variable importance in projection
- K-W Kruskal-Wallis nonparametric test
- HCA Hierarchical cluster analysis
- HMA Heat map analysis
- PCA Principal component analysis
- OPLS-DA Orthogonal partial least squares-discrimination analysis
- ATP Adenosine-triphosphate
- ABC ATP-binding cassette

Supplementary Information

The online version contains supplementary material available at <https://doi.org/10.1186/s40538-023-00512-6>.

Additional file 1: Table S1. DEMs in chamomile under different nicotine concentration (VIP > 1, p < 0.05), sorted by compound type and arranged in descending order by VIP value.

Acknowledgements

The authors express their special gratitude to all the funding sources.

Author contributions

PZ and QL contributed to conceptualization and writing—original draft preparation. DP and YZ were involved in methodology. MJ and XZ performed formal analysis. YB and XL did investigation. YD contributed to resources. GW

and NW were involved in data curation. PZ and QL were involved in writing—review and editing. YD, GW and NW supervised the study. All authors read and approved the final manuscript.

Funding

This work was supported by the National Natural Science Foundation of China (grant number 32160302/32260541/32160517/31860357), the Key Projects of Science and Technology Plan of Yunnan Branch of China Tobacco Corporation (2019530000241011), and Yunnan Fundamental Research Projects-Youth Project (202201AU070184).

Availability of data and materials

The data sets used and/or analyzed during the current study are available to readers as in the manuscript and from the corresponding author upon reasonable request.

Declarations

Ethics approval and consent to participate

Not applicable.

Consent for publication

Not applicable.

Competing interests

The authors declare that they have no competing interests.

Author details

¹Yunnan Agricultural University, Kunming 650100, China.

Received: 3 September 2023 Accepted: 21 November 2023

Published online: 30 November 2023

References

- Dai YL, Li Y, Wang Q, Niu FJ, Li KW, Wang YY, Wang J, Zhou CZ, Gao L. Chamomile: a review of its traditional uses, chemical constituents, pharmacological activities and quality control studies. *Molecules*. 2023;28:133. <https://doi.org/10.3390/molecules28010133>.
- Shakya P, Thakur R, Sharan H, Yadav N, Kumar M, Chauhan R, Kumar D, Kumar A, Singh S, Singh S. GGE biplot and regression based multi-environment investigations for higher yield and essential oil content in German chamomile (*Matricaria chamomilla* L.). *Ind Crop Prod*. 2023;193:116145. <https://doi.org/10.1016/j.indcrop.2022.116145>.
- Bączek KB, Wiśniewska M, Przybył JL, Kosakowska O, Zenon W. Arbuscular mycorrhizal fungi in chamomile (*Matricaria recutita* L.) organic cultivation. *Ind Crop Prod*. 2019;140:111562. <https://doi.org/10.1016/j.indcrop.2019.111562>.
- Catani MV, Rinaldi F, Tullio V, Gasperi V, Savini I. Comparative analysis of phenolic composition of six commercially available chamomile (*Matricaria chamomilla* L.) extracts: potential biological implications. *Int J Mol Sci*. 2021;22:10601. <https://doi.org/10.3390/ijms221910601>.
- Lencucha R, Drope J, Magati P, Sahadewo GA. Tobacco farming: overcoming an understated impediment to comprehensive tobacco control. *Tob Control*. 2022;31:308–12. <https://doi.org/10.1136/tobaccocontrol-2021-056564>.
- Zou XD, Bk A, Abu-Izneid T, Aziz A, Devnath P, Rauf A, Mitra S, Emran TB, Mujawah AAH, Lorenzo JM, Mubarak MS, Wilairatana P, Suleria HAR. Current advances of functional phytochemicals in *Nicotiana* plant and related potential value of tobacco processing waste: a review. *Biomed Pharmacother*. 2021;143:112191. <https://doi.org/10.1016/j.biopha.2021.112191>.
- Lozano A, Martínez-Uroz MA, Gómez-Ramos MJ, Gómez-Ramos MM, Mezcuza M, Fernández-Alba AR. Determination of nicotine in mushrooms by various GC/MS- and LC/MS-based methods. *Anal Bioanal Chem*. 2012;402:935–43. <https://doi.org/10.1007/s00216-011-5490-5>.
- Yarahmadi A, Zal F, Bolouki A. Protective effects of quercetin on nicotine induced oxidative stress in 'HepG2 cells'. *Toxicol Mech Method*. 2017;27:609–14. <https://doi.org/10.1080/15376516.2017.1344338>.
- Lisuma JB, Philip AJ, Ndakidemi PA, Mbega ER. Assessing residue effects of tobacco nicotine on the yields, nutrient concentrations and nicotine uptake of a subsequent maize crop. *Field Crop Res*. 2022;277:108401. <https://doi.org/10.1016/j.fcr.2021.108401>.
- Cheng YD, Bai YX, Jia M, Chen Y, Wang D, Wu T, Wang G, Yang HW. Potential risks of nicotine on the germination, growth, and nutritional properties of broad bean. *Ecotox Environ Safe*. 2021;209:111797. <https://doi.org/10.1016/j.ecoenv.2020.111797>.
- Alkhatib R, Alkhatib B, Abdo N. Impact of exogenous nicotine on the morphological, physio-biochemical, and anatomical characteristics in *Capsicum annum*. *Int J Phytoremediat*. 2021;24:666–74. <https://doi.org/10.1080/15226514.2021.1962798>.
- Göger G, Demirci B, Ilgin S, Demirci F. Antimicrobial and toxicity profiles evaluation of the Chamomile (*Matricaria recutita* L.) essential oil combination with standard antimicrobial agents. *Ind Crop Prod*. 2018;120:279–85. <https://doi.org/10.1016/j.indcrop.2018.04.024>.
- Rathore S, Kumar R. Dynamics of phosphorus and biostimulants on agromorphology, yield, and essential oil profile of German chamomile (*Matricaria chamomilla* L.) under acidic soil conditions of western Himalaya. *Front Plant Sci*. 2022;13:917388. <https://doi.org/10.3389/fpls.2022.917388>.
- Lei SH, Rossi S, Huang BR. Metabolic and physiological regulation of aspartic acid-mediated enhancement of heat stress tolerance in perennial ryegrass. *Plants*. 2022;11:199. <https://doi.org/10.3390/plants11020199>.
- Xiao Y, Liu H, Li HF, Liu QJ, Lu Q, Varshney RK, Chen XP, Hong YB. Widely targeted metabolomics characterizes the dynamic changes of chemical profile in postharvest peanut sprouts grown under the dark and light conditions. *LWT-Food Sci Technol*. 2021;152:112283. <https://doi.org/10.1016/j.lwt.2021.112283>.
- Wang T, Zhang FJ, Zhuang WB, Shu XC, Wang Z. Metabolic variations of flavonoids in leaves of *T. media* and *T. mairei* obtained by UPLC-ESI-MS/MS. *Molecules*. 2019;2021(24):3323. <https://doi.org/10.3390/molecules24183323>.
- Nie H, Chen HC, Li GL, Su KZ, Song MB, Duan ZH, Li XC, Cao XF, Huang JG, Huang SQ, Luo YH. Comparison of flavonoids and phenylpropanoids compounds in Chinese water chestnut processed with different methods. *Food Chem*. 2020;335:127662. <https://doi.org/10.1016/j.foodchem.2020.127662>.
- Zhou P, Hu Q, Fu HY, Ouyang LQ, Gong XD, Meng P, Wang Z, Dai M, Guo XM, Wang Y. UPLC-Q-TOF/MS-based untargeted metabolomics coupled with chemometrics approach for Tieguanyin tea with seasonal and year variations. *Food Chem*. 2019;283:73–82. <https://doi.org/10.1016/j.foodchem.2019.01.050>.
- Li CR, Yang LX, Guo ZF, Yang H, Zhang Y, Wang YM, Zhang GZ, Li P, Gao W. LC-MS-based untargeted metabolomics reveals chemical differences of Cannabis leaves from different regions of China. *Ind Crop Prod*. 2022;176:114411. <https://doi.org/10.1016/j.indcrop.2021.114411>.
- Li CN, Chen SX, Wang Y. Physiological and proteomic changes of *Castanopsis fissa* in response to drought stress. *Sci Rep*. 2023;13:12567. <https://doi.org/10.1038/S41598-023-39235-X>.
- Wu LL, Wang YJ, Guo PR, Li Z, Li JA, Tan XF. Metabonomic and transcriptomic analyses of *Camellia oleifera* flower buds treated with low-temperature stress during the flowering stage. *Ind Crop Prod*. 2022;189:115874. <https://doi.org/10.1016/j.indcrop.2022.115874>.
- Shi ZJ, Han XY, Wang GH, Qiu J, Zhou LJ, Chen SM, Fang WM, Chen FD, Jiang JF. Transcriptome analysis reveals chrysanthemum flower discoloration under high-temperature stress. *Front Plant Sci*. 2022;13:1003635. <https://doi.org/10.3389/fpls.2022.1003635>.
- Boyko JD, Hagen ER, Beaulieu JM, Vasconcelos T. The evolutionary responses of life-history strategies to climatic variability in flowering plants. *New Phytol*. 2023;240:1587–600. <https://doi.org/10.1111/nph.18971>.
- Yahyazadeh M, Nowak M, Kima H, Selmar D. Horizontal natural product transfer: a potential source of alkaloidal contaminants in phytopharmaceuticals. *Phytomedicine*. 2017;34:21–5. <https://doi.org/10.1016/j.phymed.2017.07.007>.
- Selmar D, Engelhardt UH, Hänsel S, Thräne C, Nowak M, Kleinwächter M. Nicotine uptake by peppermint plants as a possible source of nicotine in

- plant-derived products. *Agron Sustain Dev.* 2015;35:1185–90. <https://doi.org/10.1007/s13593-015-0298-x>.
26. Sheikhalipour M, Mohammadi SA, Esmaeelpour B, Spanos A, Mahmoudi R, Mahdavinia GR, Milani MH, Kahnamoie A, Nouraein M, Antoniou C, Kulak M, Gohari G, Fotopoulos V. Seedling nanopriming with selenium-chitosan nanoparticles mitigates the adverse effects of salt stress by inducing multiple defence pathways in bitter melon plants. *Int J Biol Macromol.* 2023;242:124923. <https://doi.org/10.1016/J.IJBIOMAC.2023.124923>.
 27. Gao YM, An TT, Kuang QQ, Wu YJ, Liu S, Liang LY, Min Y, Andrew M, Chen YL. The role of arbuscular mycorrhizal fungi in the alleviation of cadmium stress in cereals: a multilevel meta-analysis. *Sci Total Environ.* 2023;902:166091. <https://doi.org/10.1016/j.scitotenv.2023.166091>.
 28. Wang HJ, Liu SH, Wang TL, Liu HW, Xu XH, Chen KS, Zhang PY. The moss flavone synthase I positively regulates the tolerance of plants to drought stress and UV-B radiation. *Plant Sci.* 2020;298:110591. <https://doi.org/10.1016/j.plantsci.2020.110591>.
 29. Qin XY, Yin Y, Zhao JH, An W, Fan YF, Liang XJ, Cao YL. Correction to: Metabolomic and transcriptomic analysis of Lycium chinese and L. ruthenicum under salinity stress. *BMC Plant Biol.* 2022;22:8–26. <https://doi.org/10.1186/s12870-021-03375-x>.
 30. Zou JN, Yu H, Yu Q, Jin XJ, Cao L, Wang MY, Wang MX, Ren CY, Zhang YX. Physiological and UPLC-MS/MS widely targeted metabolites mechanisms of alleviation of drought stress-induced soybean growth inhibition by melatonin. *Ind Crop Prod.* 2021;163:113323. <https://doi.org/10.1016/j.indcrop.2021.113323>.
 31. Fatnani D, Patel M, Parida AK. Regulation of chromium translocation to shoot and physiological, metabolomic, and ionic adjustments confer chromium stress tolerance in the halophyte *Suaeda maritima*. *Environ Pollut.* 2023;320:121046. <https://doi.org/10.1016/j.envpol.2023.121046>.
 32. Jing YY, Liu CH, Liu BB, Pei TT, Zhan MH, Li CR, Wang DN, Li PM, Ma FW. Overexpression of the FERONIA receptor kinase *MdMRLK2* confers apple drought tolerance by regulating energy metabolism and free amino acids production. *Tree Physiol.* 2023;43:154–68. <https://doi.org/10.1093/treephys/tpac100>.
 33. He XM, Zhang J, Ren YN, Sun CY, Deng XP, Qian M, Hu ZB, Li R, Chen YH, Shen ZG, Xia Y. Polyaspartate and liquid amino acid fertilizer are appropriate alternatives for promoting the phytoextraction of cadmium and lead in *Solanum nigrum* L. *Chemosphere.* 2019;237:124483. <https://doi.org/10.1016/j.chemosphere.2019.124483>.
 34. Singh S, Parihar P, Singh R, Singh VP, Prasad SM. Heavy Metal tolerance in plants: role of transcriptomics, proteomics, metabolomics, and ionomics. *Front Plant Sci.* 2016;6:1143–67. <https://doi.org/10.3389/fpls.2015.01143>.
 35. Tan PP, Zeng CZ, Wan C, Liu Z, Dong XJ, Peng JQ, Lin HY, Li M, Liu ZX, Yan ML. Metabolic profiles of *Brassica Juncea* roots in response to cadmium stress. *Metabolites.* 2021;11:383–402. <https://doi.org/10.3390/metab111060383>.
 36. Wang YJ, Dai J, Chen R, Song C, Wei PP, Wang YL, Cai YP, Han BX. Long noncoding RNA-based drought regulation in the important medicinal plant *Dendrobium huoshanense*. *Acta Physiol Plant.* 2021;43:144. <https://doi.org/10.1007/s11738-021-03314-1>.
 37. Habib S, Lwin YY, Li N. Down-regulation of *SlGRAS10* in tomato confers abiotic stress tolerance. *Genes.* 2021;12:623–44. <https://doi.org/10.3390/genes12050623>.
 38. Dufour C, Villa-Rodríguez JA, Furger C, Lessard-Lord J, Gironde C, Rigal M, Badr A, Desjardins Y, Guyonnet D. Cellular antioxidant effect of an aronia extract and its polyphenolic fractions enriched in proanthocyanidins, phenolic acids, and anthocyanins. *Antioxidants.* 2022;11:1561–80. <https://doi.org/10.3390/antiox11081561>.
 39. Ciriello M, Formisano L, Kyriacou MC, Carillo P, Scognamiglio L, Pascale SD, Roupheal Y. Morpho-physiological and biochemical responses of hydroponically grown basil cultivars to salt stress. *Antioxidants.* 2022;11:2207–29. <https://doi.org/10.3390/antiox11112207>.
 40. Mencin M, Abramović H, Jamnik P, Mikulić PM, Veberić R, Terpinč P. Abiotic stress combinations improve the phenolics profiles and activities of extractable and bound antioxidants from germinated spelt (*Triticum spelta* L.) seeds. *Food Chem.* 2020;344:128704. <https://doi.org/10.1016/j.foodchem.2020.128704>.
 41. Chen YF, Yi N, Yao SB, Zhuang JH, Fu ZP, Ma J, Yin SX, Jiang XL, Liu YJ, Gao LP, Xia T. CsHCT-mediated lignin synthesis pathway involves in the response of tea plants to biotic and abiotic stresses. *J Agric Food Chem.* 2021;69:10069–81. <https://doi.org/10.1021/acs.jafc.1c02771>.
 42. Mehari TG, Xu YC, Umer MJ, Shiraku ML, Hou YQ, Wang YH, Yu SX, Zhang XL, Wang KB, Cai XY, Zhou ZL, Liu F. Multi-omics-based identification and functional characterization of *Gh_A06G1257* proves its potential role in drought stress tolerance in *Gossypium hirsutum*. *Front Plant Sci.* 2021;12:746771. <https://doi.org/10.3389/fpls.2021.746771>.
 43. Haghighi M, Saadat S, Abbey L. Effect of exogenous amino acids application on growth and nutritional value of cabbage under drought stress. *Sci Hortic-Amsterdam.* 2020;272:109561. <https://doi.org/10.1016/j.scienta.2020.109561>.
 44. Hollenstein K, Frei DC, Locher KP. Structure of an ABC transporter in complex with its binding protein. *Nature.* 2007;446:213–6. <https://doi.org/10.1038/nature05626>.
 45. Guo ZL, Yuan XQ, Li LY, Zeng M, Yang J, Tang H, Duan CQ. Genome-wide analysis of the ATP-binding cassette (ABC) transporter family in *Zea mays* L. and its response to heavy metal stresses. *Int J Mol Sci.* 2022;23:2109–22. <https://doi.org/10.3390/ijms23042109>.
 46. Mumtaz MA, Hao YY, Mehmood S, Shu HY, Zhou Y, Jin WH, Chen CH, Li L, Altaf MA, Wang ZW. Physiological and transcriptomic analysis provide molecular insight into 24-epibrassinolide mediated Cr (VI)-toxicity tolerance in pepper plants. *Environ Pollut.* 2022;306:119375. <https://doi.org/10.1016/j.envpol.2022.119375>.
 47. Zhang JJ, Yang H. Metabolism and detoxification of pesticides in plants. *Sci Total Environ.* 2021;790:148034. <https://doi.org/10.1016/j.scitotenv.2021.148034>.
 48. Li SJ, Liu SC, Lin XH, Grierson D, Yin XR, Chen KS. Citrus heat shock transcription factor *CitHsfA7*-mediated citric acid degradation in response to heat stress. *Plant Cell Environ.* 2021;45:95–104. <https://doi.org/10.1111/pce.14207>.
 49. Tahjib-UI-Arif M, Zahan MI, Karim MM, Imran S, Hunter CT, Islam MS, Mia MA, Hannan MA, Rhaman MS, Hossain MA, Brestic M, Skalicky M, Murata Y. Citric acid-mediated abiotic stress tolerance in plants. *Int J Mol Sci.* 2021;22:7235. <https://doi.org/10.3390/ijms22137235>.
 50. Viana EV, Aranha BC, Busanello C, Maltzahn LE, Panozzo LE, Oliveira AC, Rombaldi CV, Pegoraro C. Metabolic profile of canola (*Brassica napus* L.) seedlings under hydric, osmotic and temperature stresses. *Plant Stress.* 2022;3:100059. <https://doi.org/10.1016/j.stress.2022.100059>.
 51. Wu Y, Li Z, Zhu H, Zi R, Xue F, Yu Y. Identification of tartary buckwheat (*Fagopyrum tataricum* (L.) Gaertn) and common buckwheat (*Fagopyrum esculentum* Moench) using gas chromatography-mass spectroscopy-based untargeted metabolomics. *Foods.* 2023;12:2578. <https://doi.org/10.3390/foods12132578>.
 52. Liu L, Kong Q, Xiang Z, Kuang X, Wang H, Zhou L, Feng S, Chen T, Ding C. Integrated analysis of transcriptome and metabolome provides insight into *Camellia oleifera* oil alleviating fat accumulation in high-fat *Caenorhabditis elegans*. *Int J Mol Sci.* 2023;24(14):11615. <https://doi.org/10.3390/ijms241411615>.
 53. Aritra CR, Pankaj T, Munusamy M. ACC deaminase producing endophytic bacteria enhances cell viability of rice (*Oryza sativa* L.) under salt stress by regulating ethylene emission pathway. *Environ Exp Bot.* 2023;213:105411. <https://doi.org/10.1016/j.envexpbot.2023.105411>.
 54. Jenna L, Jan S, Pushan B. Salicylic acid metabolism and signalling coordinate senescence initiation in aspen in nature. *Nat Commun.* 2023;14(1):4288. <https://doi.org/10.1038/S41467-023-39564-5>.
 55. Yang ZH, Xue BH, Song GL, Shi SQ. Effects of citric acid on antioxidant system and carbon-nitrogen metabolism of *Elymus dahuricus* under Cd stress. *Ecotox Environ Safe.* 2022;233:113321. <https://doi.org/10.1016/j.ecoenv.2022.113321>.
 56. Li M, Li YM, Zhang WD, Li SH, Gao Y, Ai XZ, Zhang DL, Liu BB, Li QM. Metabolomics analysis reveals that elevated atmospheric CO₂ alleviates drought stress in cucumber seedling leaves. *Anal Biochem.* 2018;559:71–85. <https://doi.org/10.1016/j.ab.2018.08.020>.
 57. Krämer M, Dörfer E, Hickl D, Bellin L, Scherer V, Möhlmann T. Cytidine triphosphate synthase four from *Arabidopsis thaliana* attenuates drought stress effects. *Front Plant Sci.* 2022;13:842156. <https://doi.org/10.3389/fpls.2022.842156>.

Publisher's Note

Springer Nature remains neutral with regard to jurisdictional claims in published maps and institutional affiliations.